

Soil-structure interaction effect on active control of multi-story buildings under earthquake loads

Genda Chen[†], Chaoqiang Chen[‡] and Franklin Y. Cheng^{‡†}

*Department of Civil Engineering, University of Missouri-Rolla,
111 Butler-Carlton Hall, Rolla, MO 65409-0030, U.S.A.*

Abstract. A direct output feedback control scheme was recently proposed by the authors for single-story building structures resting on flexible soil body. In this paper, the control scheme is extended to mitigate the seismic responses of multi-story buildings. Soil-structure interaction is taken into account in two parts: input at the soil-structure interface/foundation and control algorithm. The former reflects the effect on ground motions and is monitored in real time with accelerometers at foundation. The latter includes the effect on the dynamic characteristics of structures, which is formulated by modifying the classical linear quadratic regulator based on the fundamental mode shape of the soil-structure system. Numerical results on the study of a 1/4-scale three-story structure, supported by a viscoelastic half-space of soil mass, have demonstrated that the proposed algorithm is robust and very effective in suppressing the earthquake-induced vibration in building structures even supported on a flexible soil mass. Parametric studies are performed to understand how soil damping and flexibility affect the effectiveness of active tendon control. The selection of weighting matrix and effect of soil property uncertainty are investigated in detail for practical applications.

Key words: active control; soil-structure interaction; state feedback gain; output feedback gain; soil parameter uncertainty; seismic effectiveness; robustness and sensitivity.

1. Introduction

Extensive study on active control of structures has led to actual implementations in several dozens of civil engineering structures throughout the world (Wu 1995). Nearly all control systems were designed for structures on rigid bases. In practice, however, many civil structures are supported on footings that rest on flexible soil masses. How the soil flexibility affects the performance of control algorithms is a puzzling question in the mind of engineers.

Recent studies in active structural control considering soil-structure interaction have been developed in two directions. One is to consider soil and foundation as part of an augmented soil-structure system (Cheng and Suthiwong 1996) and the other is to simplify the soil-structure system into a reduced-order structure of modified parameters by neglecting the inertia effect of the foundation component (Luco 1998, Smith *et al.* 1994). The optimal closed-loop control algorithms are then applied into the augmented or simplified system. To implement a control concept in a structure,

[†] Assistant Professor
[‡] Ph.D. Candidate
^{‡†} Curators' Professor

both sensors and actuators have to be installed physically in the structures. Therefore, in the first approach, the so-called observer technique has to be used and the dynamic responses of the soil body are estimated based on those measured on structures. From the mathematical point of view, the responses of a building structure under earthquake loadings can be uniquely determined without explicit modeling of the soil body if the complete motion at the soil-structure interface can be monitored in real time. Therefore it is not necessary to explicitly include the soil mass in an analytical model for the study of active structural control with surface foundation. In the second approach, negligence of the foundation mass in the development of control algorithms sometime leads to a considerable degradation of the algorithm performance in reducing the responses of the soil-structure system (Chen *et al.* 1999).

The objective of this paper is to study how soil damping and flexibility affect the performance of active control systems, to understand how robust active control systems are in terms of soil parameter uncertainties, and to develop a practical control scheme for multi-story building structures resting on a viscoelastic half space of soil mass. Soil-structure interaction (SSI) is taken into account in two parts: input at foundation and control algorithm. The former reflects the SSI effect on ground motions, which will be determined in real time. The latter includes the interaction effect on the dynamic characteristics of structures and is derived below.

2. Optimal feedback control of soil-structure systems

Consider a n -story building structure resting on a half space of homogeneous soil deposits as shown in Fig. 1. The structure is a viscously-damped, linear system and the soil body is a viscoelastic system.

2.1. Soil modeling

The effect of a viscoelastic soil mass on the vibration of the building structure in one direction can be characterized by two sets of springs and dashpots at the foundation, one for translational and the other for rotational movement. The foundation vibrations associated with the translational and rotational movement are referred to as lateral and rocking modes. The coupling effect between two modes is insignificant and thus neglected in this study (Veletsos and Wei 1971).

Consider a rectangular foundation of length $2L$ along the ground motion and width $2B$. When $B/L \geq 0.4$, the stiffness and damping constants of the soil mass can be expressed into (Dobry and Gazetas 1986)

$$k_y = \bar{k}_y(\omega) \left[\frac{9(B/L)^{0.38}}{2-\nu} - \frac{0.21}{0.75-\nu} \left(1 - \frac{B}{L} \right) \right] L \rho_s V_s^2 - 4\bar{c}_y(\omega) \xi_s \omega \rho_s V_s B L \quad (1)$$

$$c_y = 4\bar{c}_y(\omega) \rho_s V_s B L + 2\bar{k}_y(\omega) \xi_s \left[\frac{9(B/L)^{0.38}}{2-\nu} - \frac{0.21}{0.75-\nu} \left(1 - \frac{B}{L} \right) \right] L \rho_s V_s^2 / \omega \quad (2)$$

for lateral mode and

$$k_\theta = \bar{k}_\theta(\omega) \cdot \frac{25.6 \rho_s V_s^2}{1-\nu} \cdot \left(\frac{B L^3}{12} \right)^{0.75} - \bar{c}_\theta(\omega) \cdot \frac{54.4 \rho_s V_s}{\pi(1-\nu)} \cdot \frac{B L^3}{12} \xi_s \omega \quad (3)$$

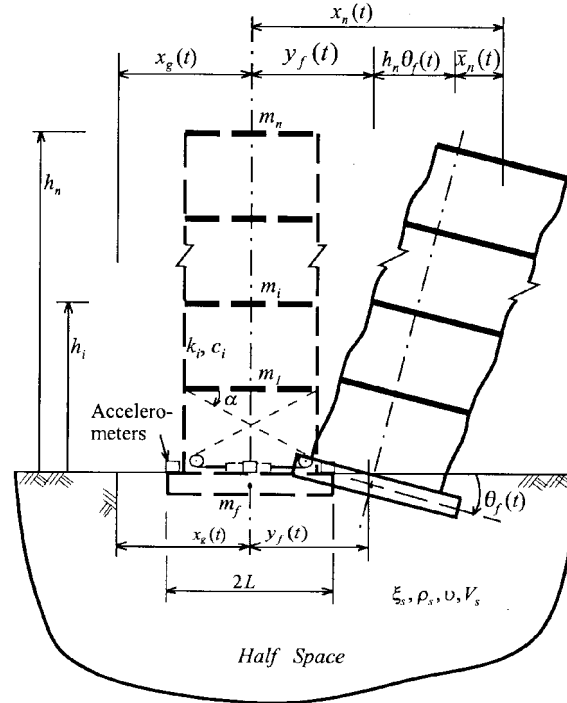


Fig. 1 Schematic of soil-structure system

field motion of earthquake.

2.3. State feedback control

In the state space, Eq. (5) can be written into

$$\dot{Z}(t) = AZ(t) + Bu(t) + H\ddot{x}_g(t) \tag{6}$$

where

$$Z(t) = \begin{Bmatrix} X(t) \\ \dot{X}(t) \end{Bmatrix}, \quad A = \begin{bmatrix} \mathbf{O} & \mathbf{I} \\ -\mathbf{M}^{-1}\mathbf{K} & -\mathbf{M}^{-1}\mathbf{C} \end{bmatrix}, \quad B = \begin{Bmatrix} \mathbf{O} \\ \mathbf{M}^{-1}\mathbf{D} \end{Bmatrix} \quad \text{and} \quad H = \begin{Bmatrix} \mathbf{O} \\ -\mathbf{E} \end{Bmatrix}.$$

The performance index (PI) for control of building responses in this study is described by

$$J = \int_0^{t_f} [Z^T(t)QZ(t) + \beta k_1 u^2(t)] dt \tag{7}$$

in which Q is a $2(n+2) \times 2(n+2)$ dimensional weighting matrix. The coefficient β determines the relative importance of control effectiveness (response reduction) and economy (control force requirements). $\beta = \infty$ represents the uncontrolled case. The quantity t_f is the terminal time which covers the entire duration of strong earthquake motion. Following the standard optimization procedure (Soong 1990), the closed-loop control force to minimize the PI in Eq. (7) can be expressed into

$$\mathbf{u}(t) = \mathbf{GZ}(t) = -\frac{1}{2\beta k_1} \mathbf{B}^T \mathbf{PZ}(t) \quad (8)$$

in which \mathbf{P} is a Riccati matrix, satisfying the following matrix Riccati equation

$$\mathbf{PA} - \frac{1}{2\beta k_1} \mathbf{PBB}^T \mathbf{P} + \mathbf{A}^T \mathbf{P} + 2\mathbf{Q} = 0 \quad (9)$$

3. Proposed output feedback control

The control force in state feedback control, described by Eq. (8), is a function of the displacement and velocity at foundation with respect to the free field motion of earthquake. Unfortunately this information is not available in practical applications of structural control. What can be obtained in real time is the absolute acceleration at footing foundation. Three accelerometers are considered to be attached to the top surface of the foundation as schematically shown in Fig. 1. One is located at the center of foundation to measure the horizontal acceleration. The other two are installed at two sides of the foundation to measure vertical accelerations from which the rocking acceleration of the foundation can be determined in real time. In what follows, an output feedback law is proposed using the measurable acceleration responses at the foundation and the state responses of the building.

The control force described by Eq. (8) can be expanded into

$$\mathbf{u}(t) = \mathbf{G}_{x_s} \cdot \mathbf{X}_s(t) + \mathbf{G}_{x_f} \cdot \mathbf{X}_f(t) + \mathbf{G}_{\dot{x}_s} \cdot \dot{\mathbf{X}}_s(t) + \mathbf{G}_{\dot{x}_f} \cdot \dot{\mathbf{X}}_f(t) \quad (10)$$

in which $\mathbf{X}_s(t)$ and $\mathbf{X}_f(t)$ represent the displacements of structure and footing, respectively; $\dot{\mathbf{X}}_s(t)$ and $\dot{\mathbf{X}}_f(t)$ are the corresponding velocities relative to the free field motion. By substituting Eq. (10) into Eq. (5), the equations of motion of footing can be expressed into

$$\mathbf{T}_1 \mathbf{X}_f(t) = -\mathbf{T}_2 \ddot{\mathbf{X}}_a(t) - \mathbf{T}_3 \dot{\mathbf{X}}_f(t) - \mathbf{T}_4 \dot{\mathbf{X}}_s(t) - \mathbf{T}_5 \mathbf{X}_s(t) \quad (11)$$

where $\ddot{\mathbf{X}}_a(t) = [\ddot{\theta}_f(t) \ddot{y}_f(t) + \ddot{\mathbf{x}}_g(t)]^T$ denotes the absolute acceleration of footing. The matrices \mathbf{T}_i ($i=1, 2, 3, 4, 5$) are given in the Appendix. Solving $\mathbf{X}_f(t)$ from Eq. (11) and introducing it into Eq. (10) leads to

$$\mathbf{u}(t) = (\mathbf{G}_{x_s} - \mathbf{G}_{x_f} \mathbf{T}_1^{-1} \mathbf{T}_5) \mathbf{X}_s(t) + (\mathbf{G}_{\dot{x}_s} - \mathbf{G}_{x_f} \mathbf{T}_1^{-1} \mathbf{T}_4) \dot{\mathbf{X}}_s(t) - \mathbf{G}_{x_f} \mathbf{T}_1^{-1} \mathbf{T}_2 \ddot{\mathbf{X}}_a(t) + (\mathbf{G}_{\dot{x}_f} - \mathbf{G}_{x_f} \mathbf{T}_1^{-1} \mathbf{T}_3) \dot{\mathbf{X}}_f \quad (12)$$

It is well known that SSI tends to reduce the natural frequencies of a soil-structure system. As a result, the contribution of the fundamental mode to the total responses of the system usually increases as the soil medium gets more flexible. It is therefore reasonable to approximately estimate the foundation velocity from those of the structure by using the first mode shape. Let Φ_1 denote the mode vector of the first mode of the uncontrolled soil-structure system. The velocity response of the system can thus be approximately expressed into

$$\dot{\mathbf{X}}(t) \approx \Phi_1 \dot{q}_1(t) \quad (13)$$

Pre-multiplying $\Phi_1^T \mathbf{M}$ on both sides of Eq. (13) leads to

$$\dot{q}_1(t) \approx \frac{\Phi_1^T \mathbf{M} \dot{\mathbf{X}}(t)}{\Phi_1^T \mathbf{M} \Phi_1} \quad (14)$$

Both Φ_1 and $\dot{X}(t)$ can be partitioned into structure and foundation parts:

$$\Phi_1 = \begin{Bmatrix} \Phi_{1s} \\ \Phi_{1f} \end{Bmatrix} \text{ and } \dot{X}(t) = \begin{Bmatrix} \dot{X}_s(t) \\ \dot{X}_f(t) \end{Bmatrix} \quad (15)$$

The velocity response of footing can then be determined by

$$\dot{X}_f(t) \approx \Phi_{1f} q_1(t) = \Phi_{1f} \cdot \frac{\Phi_1^T M \dot{X}(t)}{\Phi_1^T M \Phi_1} \quad (16)$$

or

$$\dot{X}_f(t) \approx \frac{1}{\Phi_1^T M \Phi_1} \left(I - \frac{\Phi_{1f} \Phi_{1f}^T M_f}{\Phi_1^T M \Phi_1} \right)^{-1} \Phi_{1f} \Phi_{1s}^T M_s \dot{X}_s(t) = \Gamma \dot{X}_s(t) \quad (17)$$

In the equation above, Γ is a transformation matrix that is introduced to estimate the velocity response of footing. M_s and M_f are the mass matrices of the building and foundation. Both are submatrices of M .

By substituting Eq. (17) into Eq. (12), the control force can directly be calculated from the measurable accelerations at footing and state responses of the structure using

$$u(t) = G_1 X_s(t) + G_2 \dot{X}_s(t) + G_3 \ddot{X}_a(t) \quad (18)$$

in which $G_1 = G_{x_s} - G_{x_f} T_1^{-1} T_5$, $G_2 = G_{x_s} - G_{x_f} T_1^{-1} T_4 + (G_{x_f} - G_{x_f} T_1^{-1} T_3) \Gamma$ and $G_3 = -G_{x_f} T_1^{-1} T_2$. Eq. (18) is the output feedback control algorithm proposed in this paper.

4. SSI effect on active control efficiency

Previous studies in structural control were focused on reducing the peak responses of structures fixed at base. How the soil flexibility affects the performance of active control is of practical interest but not yet addressed. Limited studies by Luco (1998) and Smith *et al.* (1994) only conducted parametric analyses in the frequency domain. In addition, the variation in soil properties and the uncertainty involved in the measurement of these parameters are significantly larger than those of building structures. Sensitivity of a control algorithm to the uncertainty of soil parameters needs to be studied before the algorithm can be applied into practice. In what follows, practical issues such as the selection of the weighting matrix and the effect of soil parameter uncertainty on the performance of control designs as well as the effect of soil material damping and flexibility are discussed.

To perform a parametric study, a 1/4-scale three-story structure is used as an example. The steel frame structure has a lumped mass of 593 kg, 590 kg and 576 kg, respectively, at the first, second and third floor. It has the interval stiffness of 542, 2998 and 1298 kN/m, and a damping coefficient of 0.271, 0.0693 and 0.121 kN.sec/m, correspondingly. The natural frequencies of the structure are 16.47, 56.60 and 109.7 rad/sec with corresponding modal damping ratios of 0.364, 0.354 and 0.267%. Three floors are respectively 1.016, 1.778 and 2.54 meters above a 1.524×0.762 m rectangular footing. The foundation is made of 0.4572 m thick reinforced concrete. Therefore, the

mass and moment of inertia of the footing are 130 kg and 25.2 kg·m². The soil material filling the half space below the foundation has a Poisson's ratio of 0.33 and density of 15.7 kN/m³. The soil-structure system is subjected to the free field motion at ground surface. The NS component of the El Centro, California earthquake of May 18, 1940 is used as ground acceleration with its magnitude adjusted to a peak value of 0.98 m/sec².

When the shear wave velocity in soil decreases from infinity to 25.4 m/sec, the dimensionless factor ($\omega_1 B/V_s$, ω_1 is the fundamental frequency of the structure fixed at base) increases from 0 to 0.247. Correspondingly, the fundamental frequency of the uncontrolled soil-structure system ($\beta = \infty$) reduces by 35% and, the modal damping ratio increases almost 10 times for $\xi_s = 0.05$ and 15 times for $\xi_s = 0.10$ as shown in Tables 1 to 3. It is noted that small values have been assigned to the soil shear wave velocities due to the scale of the model structure.

4.1. Selection of weighting matrix

Three weighting matrices have been selected by Wu (1995) to minimize the potential, kinetic and mechanical energy of a single-story frame structure. It was concluded that these matrices lead to nearly the same performance of corresponding algorithms when the coefficient β in Eq. (7) correspondingly takes the value of r_0 , r_0 and $2r_0$ (r_0 is an arbitrary number).

Similar weighting matrices are considered herein. However, the purpose of installing an active

Table 1 Fundamental frequency of soil-structure system: $\xi_s = 0.05$

$\frac{\omega_1 \beta}{V_s}$	Fundamental Frequency (rad/sec)			
	$\beta=1$	$\beta=10$	$\beta=700$	$\beta=\infty$
0.000	20.18	17.50	16.49	16.47
0.124	17.65	15.39	14.40	14.37
0.247	12.23	11.21	10.67	10.63

Table 2 Damping ratio of soil-structure system: $\xi_s = 0.05$

$\frac{\omega_1 \beta}{V_s}$	Damping Ratio (%)			
	$\beta=1$	$\beta=10$	$\beta=700$	$\beta=\infty$
0.000	66.47	29.07	3.93	0.36
0.124	33.61	19.93	3.32	1.50
0.247	10.62	10.08	3.85	3.50

Table 3 Damping ratio of soil-structure system: $\xi_s = 0.10$

$\frac{\omega_1 \beta}{V_s}$	Damping Ratio (%)			
	$\beta=1$	$\beta=10$	$\beta=700$	$\beta=\infty$
0.000	66.47	29.07	3.93	0.36
0.124	32.62	20.00	3.96	2.38
0.247	12.46	11.34	5.70	5.45

control system is to reduce the structural deformation, $\bar{x}(t)$ in Fig. 1, instead of displacement $x(t)$ in Eq. (5). They are linearly related in the following way

$$\bar{x}_i(t) = -y_f(t) - h_i \theta_f(t) + x_i(t) \quad (i=1, 2, \dots, n) \quad (19)$$

In matrix form, Eq. (19) can be written as

$$\bar{\mathbf{X}}(t) = \mathbf{S} \cdot \mathbf{X}(t) \quad (20)$$

where

$$\mathbf{S} = \begin{bmatrix} 1 & 0 & \cdot & \cdot & 0 & -h_1 & -1 \\ 0 & 1 & \cdot & \cdot & 0 & -h_2 & -1 \\ \cdot & \cdot & \cdot & \cdot & \cdot & \cdot & \cdot \\ 0 & 0 & \cdot & \cdot & 1 & -h_n & -1 \end{bmatrix}. \quad (21)$$

Therefore three weighting matrices corresponding to potential, kinetic and mechanical energy are respectively expressed into

$$\mathbf{Q}_P = \begin{bmatrix} \mathbf{S}^T \mathbf{K}_s \mathbf{S} & 0 \\ 0 & 0 \end{bmatrix}, \quad \mathbf{Q}_K = \begin{bmatrix} 0 & 0 \\ 0 & \mathbf{S}^T \mathbf{M}_s \mathbf{S} \end{bmatrix} \quad \text{and} \quad \mathbf{Q}_M = \begin{bmatrix} \mathbf{S}^T \mathbf{K}_s \mathbf{S} & 0 \\ 0 & \mathbf{S}^T \mathbf{M}_s \mathbf{S} \end{bmatrix} \quad (22)$$

in which \mathbf{K}_s (a submatrix of \mathbf{K}) is the stiffness matrix of the structure fixed at base.

The performance index, the maximum acceleration and the maximum displacement are normalized by their corresponding quantities of the uncontrolled soil-structure system ($\beta = \infty$). They are presented in Figs. 2 and 3 to illustrate the influence of weighting matrix on the control effectiveness for two types of soil conditions. The three matrices in Eq. (22) are used, and their effects are compared under the constraint of equal maximum control force. It can be seen that one selection of weighting matrix does not lead to significantly more reduction of structural responses than another. This observation is especially true for flexible soil conditions. For the rest of paper, \mathbf{Q}_P is always used for this reason.

4.2. Effect of soil parameters

To show the effect of soil damping on the control efficiency, the drift time history in the first story is plotted in Fig. 4 for $\xi_s = 0.05$ and 0.10 at two levels of control force. It can be observed that both responses have the same pitch at each level of control force. However, the maximum drift decreases as soil damping increases regardless of the level of control force. This result agrees with previous studies on the SSI effect on uncontrolled structures. To understand whether this result can be generalized for cases of various soil flexibility, Tables 2 and 3 include the damping ratio of the controlled soil-structure system. As one can see, the total damping of the soil-structure system generally increases as soil damping changes from 0.05 to 0.10 . The exception to this is the case with $\beta = 1$ and $\omega_1 B/V_s = 0.124$, which indicates a large control force acted upon a structure supported on a relatively-stiff soil mass. Under these circumstances, damping due to active control constitutes a major portion of the total damping of the soil-structure system. An increase in soil damping results in a reduction in total damping. Consequently, the drift in the first story is expected

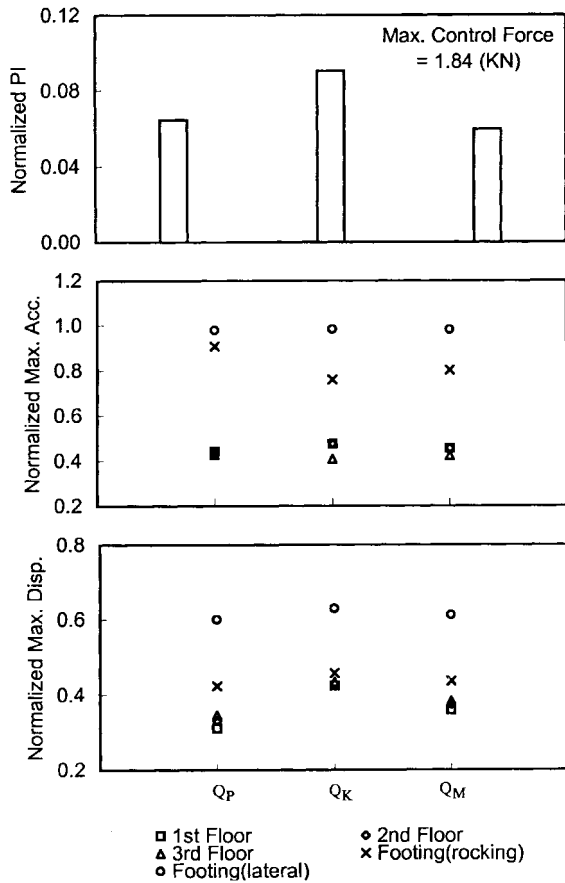


Fig. 2 Effect of weighting matrix on control effectiveness under constant max. control force: $\omega_1 B/V_s = 0.124$ and $\xi_s = 0.05$

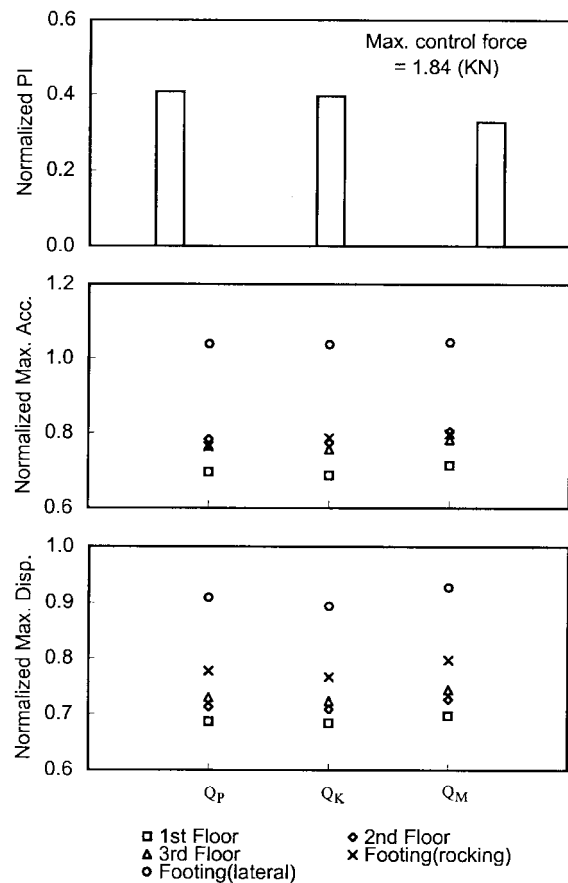


Fig. 3 Effect of weighting matrix on control effectiveness under constant max. control force: $\omega_1 B/V_s = 0.247$ and $\xi_s = 0.05$

to slightly increase in this case.

Presented in Fig. 5 are the normalized performance index and the maximum acceleration and displacement responses of the soil-structure system. They were computed under equal control force and plotted as a function of the dimensionless factor ($\omega_1 B/V_s$) to study the influence of soil flexibility. It can be clearly seen that the performance index and structural response increase as soil material softens. Specifically, the reduction in peak acceleration at the 2nd floor due to the active tendon control decreases from 70% to 20% and that in peak displacement decreases from 85% to 30% when the dimensionless factor increases from 0 to 0.247. This decrease indicates significant degrading of the control effectiveness. The exception for the above trend is the footing accelerations. The translational/horizontal acceleration nearly remains constant due to the dominance of the free field motion. The rocking acceleration at the footing can be suppressed when the soil material is not very stiff.

To further study the soil flexibility effect, time histories of the drift in the first story and the accelerations at the 3rd floor and foundation are shown in Fig. 6 for very soft and stiff soil conditions. One can see from this figure that, in addition to significant deviation in magnitude, the

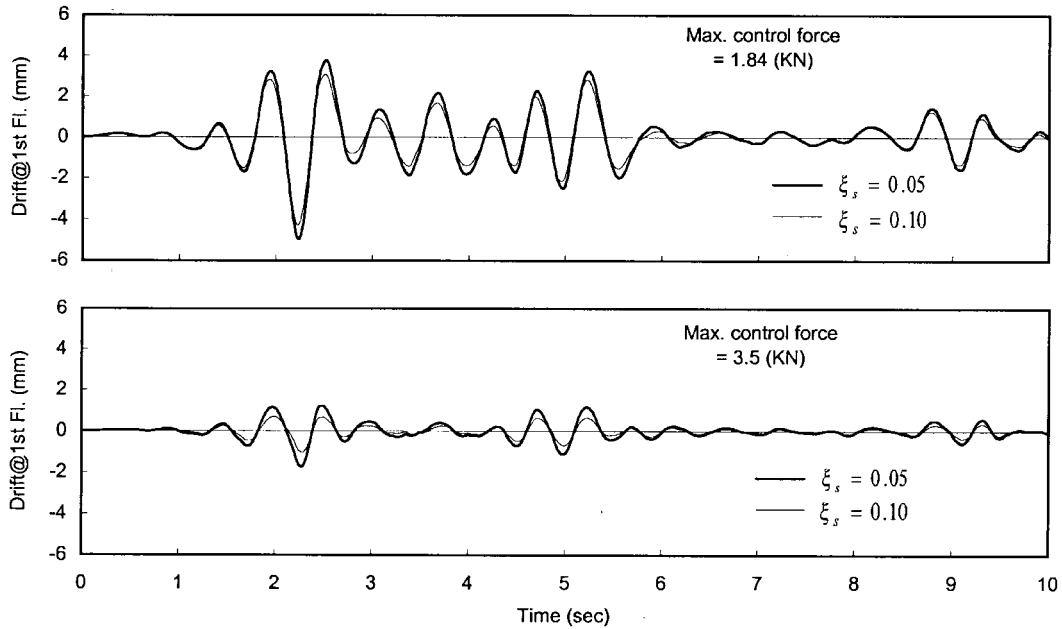


Fig. 4 Effect of soil damping on story drift: $\omega_1 B/V_s = 0.247$

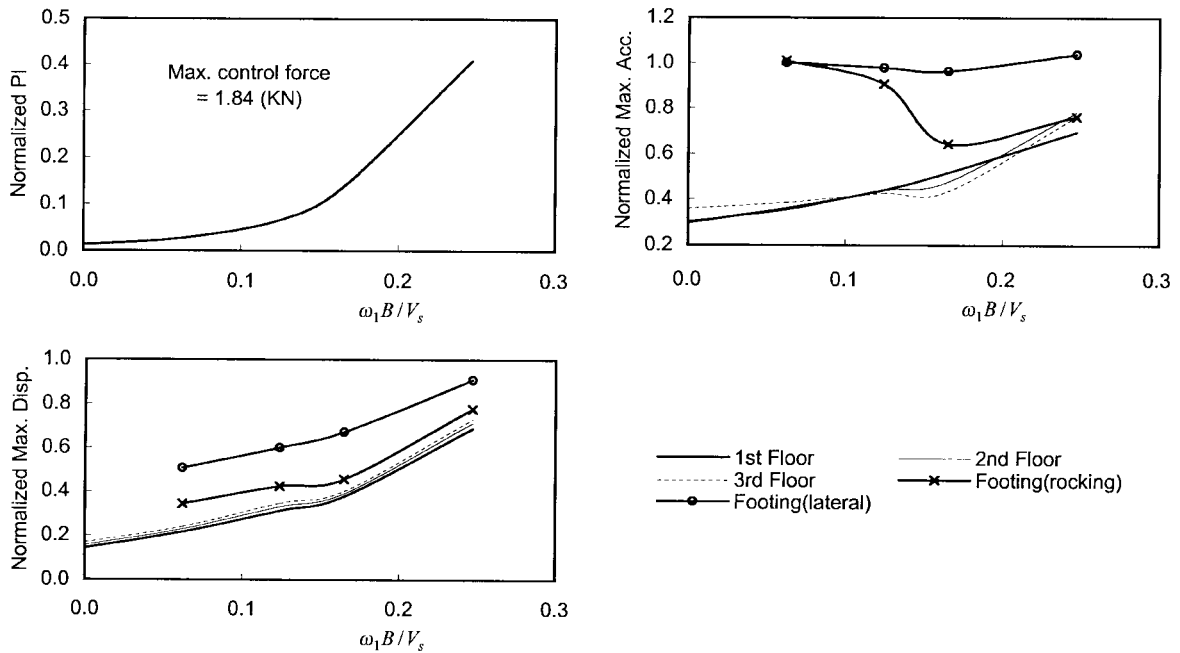


Fig. 5 SSI effect on control effectiveness under constant max. control force: $\xi_s = 0.05$

pitch of vibration also differs appreciably. This difference is attributable to the reduction in natural frequency of the soil-structure system as the soil material becomes softer as evidenced from Table 1. It

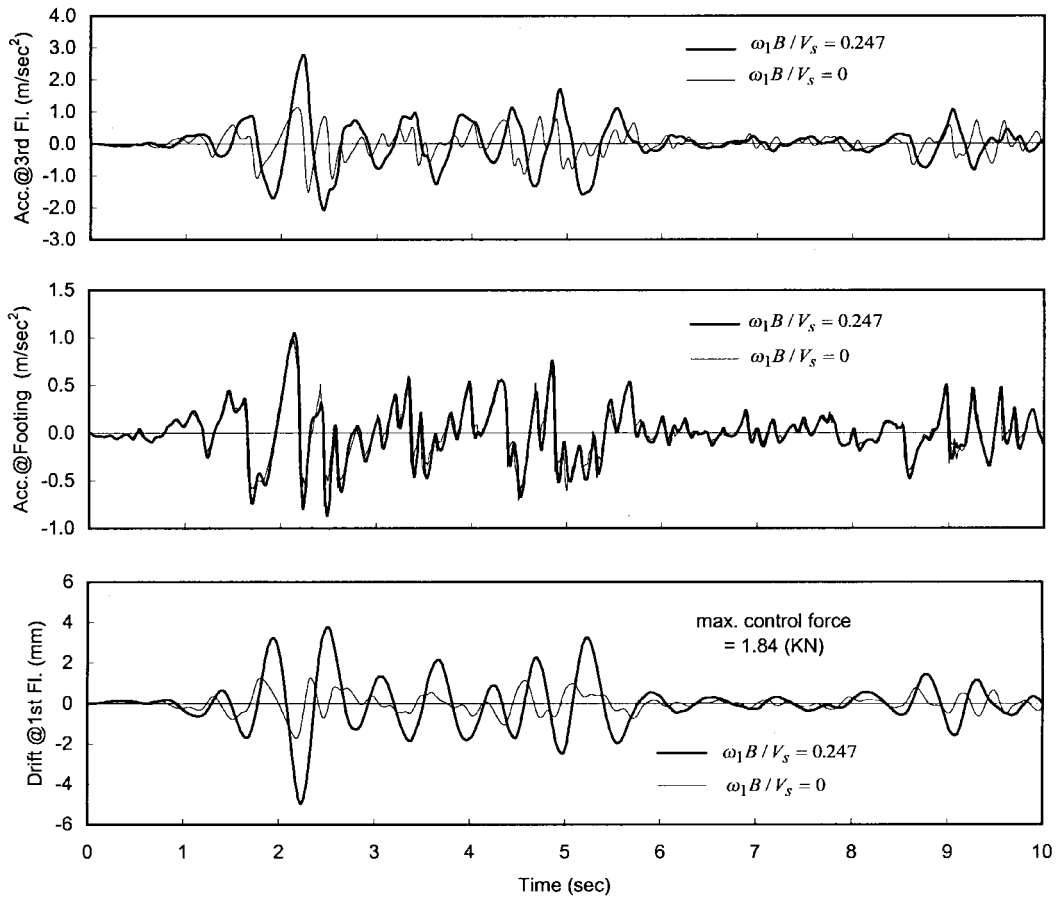


Fig. 6 Time history responses of three-story structure controlled with constant max. force: $\xi_s = 0.05$

is worth noting that the horizontal acceleration at the footing does not change significantly and the time history corresponding to a rigid base is the input to the soil-structure system.

Another way to evaluate the effectiveness of active control on a flexibly-based structure is to compare the equivalent dynamic property of the controlled structure with those of the uncontrolled structure as given in Tables 2 and 3. When $\xi_s = 0.05$, the equivalent damping increases due to active control from 0.36% to 66.47% for a rigid base while that only increases from 3.50% to 10.62% for a flexible base ($\omega_1 B/V_s = 0.247$). This indicates the tremendous reduction in total damping of the soil-structure system and thus results in less effective control on structural responses as discussed in the preceding paragraph. Indeed, the total damping of the controlled soil-structure system considerably decreases as the soil material is softening while the damping of the uncontrolled system significantly increases. At $\beta = 700$, the combined contribution of soil damping and active control results in nearly-constant system damping for various soil flexibility. It is noted that the fundamental frequency of the system increases as a result of control effort and decreases with the softening of soil mass.

4.3. Effect of soil parameter uncertainty

Uncertainties in the measurement of soil parameters are considerably larger than those associated with structural properties. In order to develop a practical control scheme for soil-structure systems, a proposed algorithm should be robust and insensitive to any unexpected uncertainty in the system property. Consider a site with a dimensionless factor ($\omega_1 B/V_s$) ranging from 0.062 to 0.247. The statistical average factor at the site is taken to be 1.24. A control algorithm can then be designed based on the average value. To see how sensitive the so-designed algorithm is to the change of soil flexibility, the performance index as well as the maximum acceleration and displacement of the soil-structure system controlled with such an algorithm are respectively divided by those corresponding to the average factor. The ratios of these responses are plotted as a function of the dimensionless factor in Fig. 7 with various lines. For the sake of comparison, the same ratios calculated with a control algorithm corresponding to the actual soil shear wave velocities are presented in Fig. 7 with solid marks. It can be observed that the control algorithm is not very sensitive to the uncertainty in soil flexibility as long as the actual soil property is in the neighborhood of the average value. The horizontal acceleration at footing nearly remains constraint due to the dominant effect of the ground motion as discussed before. The rotational acceleration and displacements at the footing progressively deviate from those based on the actual soil property as the dimensionless factor increases. They are more sensitive to the higher $\omega_1 B/V_s$ value. Therefore using a higher $\omega_1 B/V_s$

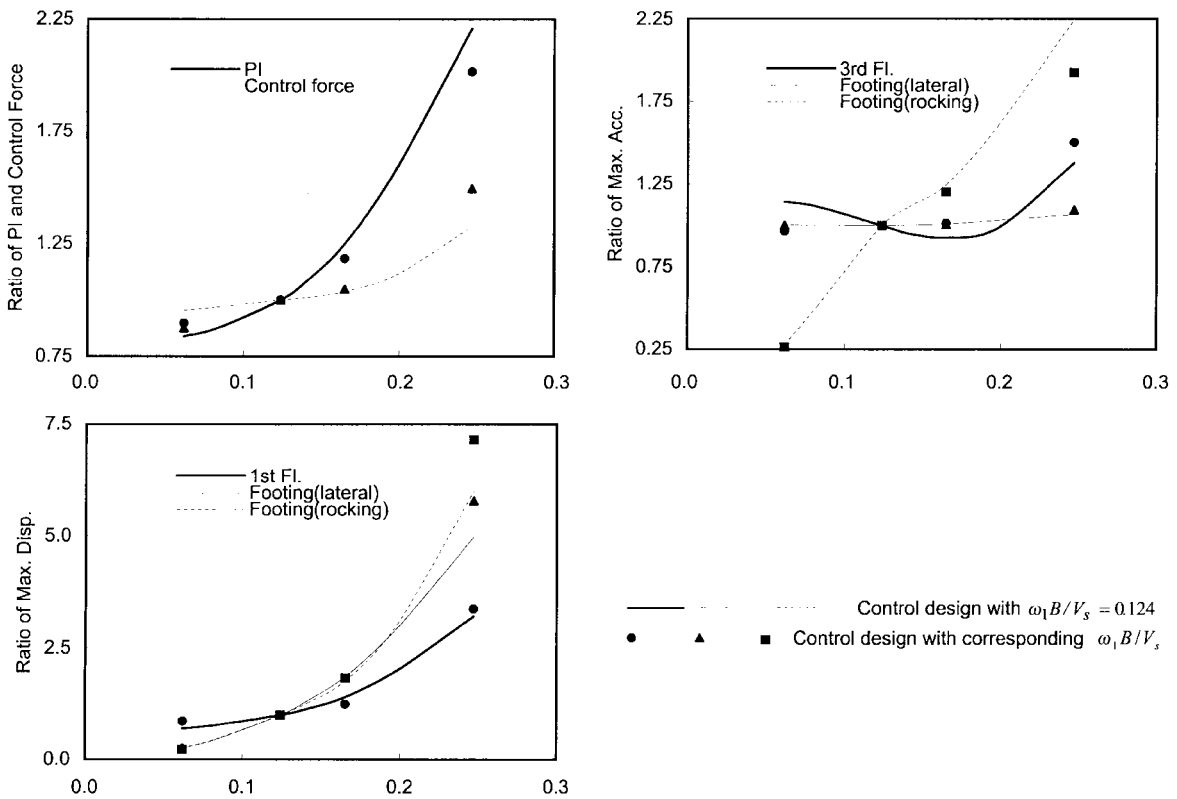


Fig. 7 Sensitivity of control algorithms to soil property uncertainty: $\xi_s = 0.05$

value to design the algorithm could slightly reduce the deviation. However, structural displacement and acceleration seem insensitive to the uncertainty in soil parameters. It can thus be concluded that the state feedback control is robust and effective in reducing the peak responses in building structures even though strong soil-structure interaction exists.

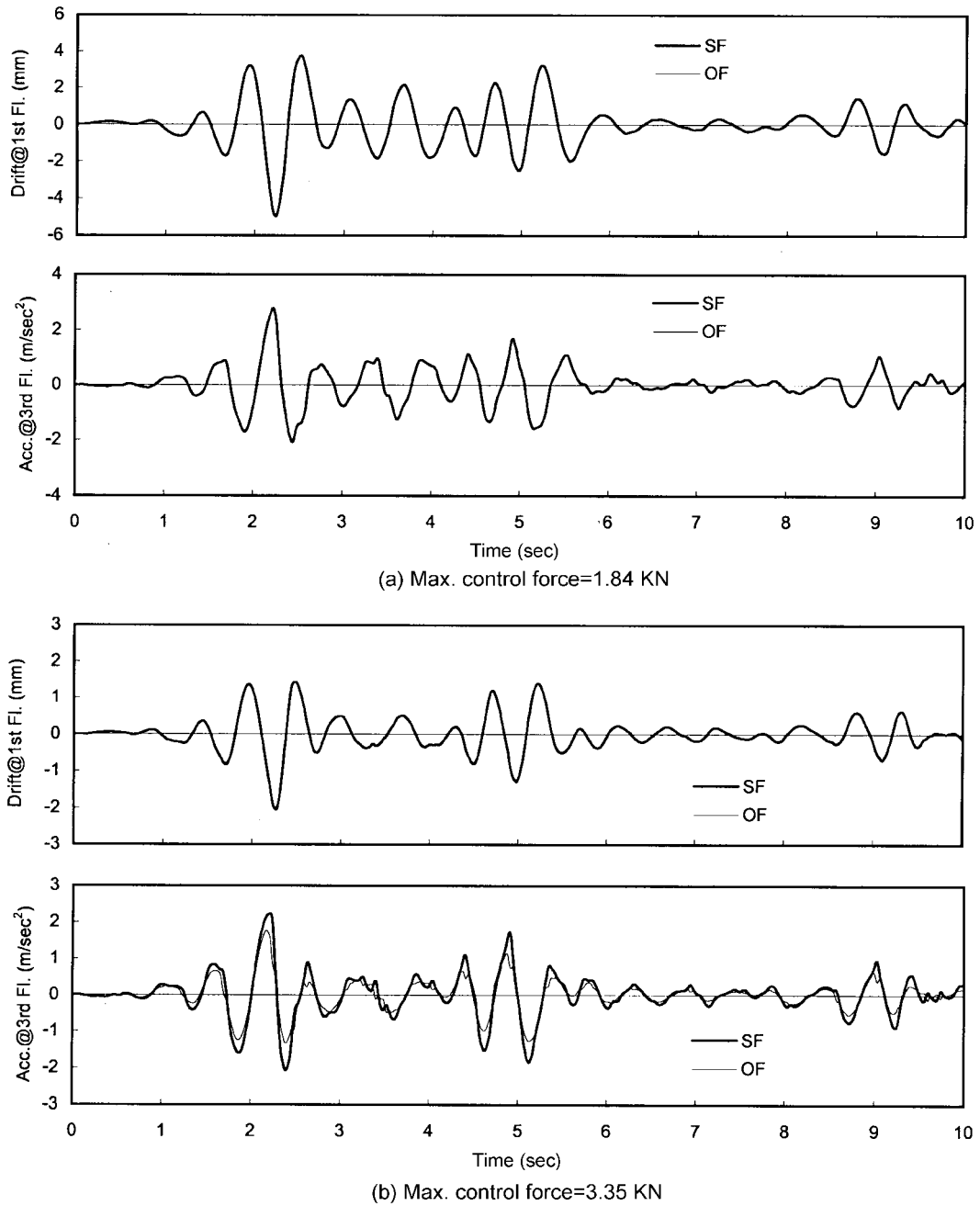


Fig. 8 Performance of various algorithms: $\omega_1 B/V_s = 0.247$ and $\xi_s = 0.05$

5. Seismic effectiveness of the proposed output control algorithm

The same example soil-structure system and earthquake input as used in Section 4 are considered to demonstrate the control efficiency of the proposed algorithm. The drifts in the 1st story and the absolute accelerations at the 3rd floor, calculated by using the state feedback (SF) and the proposed output feedback (OF) algorithm, are compared in Fig. 8 under the same control force (peak value). Fig. 8(a) clearly demonstrates that both drift and acceleration time histories using the OF algorithm coincide with those using the SF algorithm at the level of 1.84 kN control force or about 11% of the total structure weight. Therefore the proposed algorithm performs as well as the optimal control algorithm under low control forces. Even at the higher level of control force in Fig. 8(b), the two algorithms result in slightly-different drift and acceleration time histories only in magnitude. The high accuracy of the proposed algorithm is achieved because the only approximation used in the derivation of the OF algorithm is the velocity relation between the structure and foundation, Eq. (17). This approximation mainly changes the damping of the soil-structure system. In addition, the difference in acceleration is more significant than that in displacements of the controlled structure since acceleration is affected more by the higher modes.

It is observed from Fig. 8(b) that the absolute acceleration at the 3rd floor is reduced more by using the proposed OF algorithm. This reduction is likely caused by the non-optimality of the SF control due to neglecting the external disturbance in the derivation of the closed-loop algorithms, and the indirect control on acceleration in the performance index as implied by the weighting matrix in Eq. (22). A closer look at the SF-controlled soil-structure system indicates that the fundamental frequency of the system is 12.23 rad/sec as given in Table 1 for $\beta=1$. It turns out that this frequency is in the proximity of the dominant frequency of El Centro Earthquake. In addition, the earthquake record reaches its maximum ground acceleration in a short period. The combination of the nearly-resonant system and the rapidly-increasing disturbance leads to the worst performance of the SF control (Chen 2000).

6. Conclusions

A simple soil model is used to investigate the effect of soil damping and flexibility on the seismic effectiveness of active control of multi-story building structures. The influence of uncertainty in the measurement of soil parameters has been extensively studied. A practical algorithm toward the actual implementation of optimal control is then proposed, taking into account the soil-structure interaction in a simple way. Based on the extensive analyses on a three-story frame structure, the following conclusions can be drawn:

1) The fundamental frequency of a soil-structure system, controlled or uncontrolled, significantly decreases as soil material softens. However, it increases by 15% to 23% with significant control effort ($\beta=1$).

2) The damping ratio of the first mode of an uncontrolled soil-structure system significantly increases with the softening of soil material while that of the system controlled with significant effort decreases. This indicates the considerable degrading in performance of an active control system. Soil material damping plays an important role in reducing the dynamic responses of structures on flexible bases regardless of the level of control force.

3) Under the same control force (peak value), the selection of weighting matrix does not

significantly affect the amount of peak response reduction. Therefore, the weighting matrix leading to the minimization of potential energy is recommended for practical applications.

4) Uncertainty in soil parameters does not appear to significantly degrade the performance of a state feedback control algorithm as long as the algorithm is designed based on the average soil properties at a site.

5) The proposed output feedback algorithm does not require the design of an observer. It is proved very effective in reducing the maximum responses of structures. It has nearly the same performance as the full state feedback algorithm under the same control force (peak value).

Acknowledgements

The financial support from the National Science Foundation under Grant No. CMS-9733123 and Grant No. CMS 9903136 as well as the University of Missouri Research Board is gratefully acknowledged. The results, opinions and conclusions expressed in this paper are solely those of the authors and do not necessarily represent those of the sponsors.

References

- Chen, Genda. (2000), "Closed-open-loop optimal control of building structures subjected to exponentially attenuating harmonic loading", *Proceedings of the 12th World Conference on Earthquake Engineering*, Jan. 30-Feb. 4, Auckland, New Zealand.
- Chen, Genda., Chen, Chaoqiang., Lou, Menglin. and Cheng, F.Y. (1999), "Implicit vs explicit soil modeling in active structural control considering soil-structure interaction", *Proceedings of the First International Conference on Advances in Structural Engineering & Mechanics*, August 23-25, Seoul, Korea.
- Cheng, F.Y. and Suthiwong, S. (1996), "Active control for seismic-resistant structures on embedded foundation in layered half space", NSF Report, U.S. Department of Commerce, National Technical Information Service, Springfield, VA, NTIS NO. PB97-121354.
- Dobry, R. and Gazetas, G. (1986), "Dynamic response of arbitrarily shaped foundation", *J. Geotech. Engrg., ASCE*, **112**(2), 109-135.
- Luco, J.E. (1998), "A simple model for structural control including soil-structure interaction effects", *Earthquake Engrg. Struct. Dyn.*, **27**, 225-242.
- Smith, H.D., Wu, W.H. and Borja, R.I. (1994), "Structural control considering soil-structure interaction effects", *Earthquake Engrg. Struct. Dyn.*, **23**, 609-626.
- Soong, T.T. (1990), *Active Structural Control: Theory and Practice*, Longman Scientific & Technical, England.
- Veletsos, A.S. and Wei, Y.T. (1971), "Lateral and rocking vibration of footings", *J. Soil Mech. Foundations Div.*, **97**(9), 1227-1248.
- Wu, Zaiquang. (1995), "Nonlinear feedback strategies in active structural control", Ph.D. Dissertation, Department of Civil Engineering, State University of New York at Buffalo, Buffalo, NY.

Appendix: Matrices, T_i ($i = 1, 2, 3, 4, 5$)

$$T_1 = \begin{bmatrix} k_\theta + \sum_{i=1}^n k_i l_i^2 & k_1 l_1 \\ k_1 l_1 & k_y + k_1 \end{bmatrix} - 4k_c \cos \alpha \begin{Bmatrix} l_1 \\ 1 \end{Bmatrix} \mathbf{G}_{x_f} \quad (\text{A-1})$$

$$\mathbf{T}_2 = \begin{bmatrix} \mathbf{J}_f + \sum_{i=1}^n \mathbf{J}_i & 0 \\ 0 & \mathbf{m}_f \end{bmatrix} \quad (\text{A-2})$$

$$\mathbf{T}_3 = \begin{bmatrix} \mathbf{c}_\theta + \sum_{i=1}^n \mathbf{c}_i l_i^2 & \mathbf{c}_1 l_1 \\ \mathbf{c}_1 l_1 & \mathbf{c}_y + \mathbf{c}_1 \end{bmatrix} - 4\mathbf{k}_c \cos \alpha \begin{Bmatrix} l_1 \\ 1 \end{Bmatrix} \mathbf{G}_{x_f} \quad (\text{A-3})$$

$$\mathbf{T}_4 = \begin{bmatrix} \mathbf{c}_2 l_2 - \mathbf{c}_1 l_1 & \mathbf{c}_3 l_3 - \mathbf{c}_2 l_2 & \dots & \mathbf{c}_n l_n - \mathbf{c}_{n-1} l_{n-1} & -\mathbf{c}_n l_n \\ -\mathbf{c}_1 & 0 & \dots & 0 & 0 \end{bmatrix} - 4\mathbf{k}_c \cos \alpha \begin{Bmatrix} l_1 \\ 1 \end{Bmatrix} \mathbf{G}_{x_s} \quad (\text{A-4})$$

$$\mathbf{T}_5 = \begin{bmatrix} \mathbf{k}_2 l_2 - \mathbf{k}_1 l_1 & \mathbf{k}_3 l_3 - \mathbf{k}_2 l_2 & \dots & \mathbf{k}_n l_n - \mathbf{k}_{n-1} l_{n-1} & -\mathbf{k}_n l_n \\ -\mathbf{k}_1 & 0 & \dots & 0 & 0 \end{bmatrix} - 4\mathbf{k}_c \cos \alpha \begin{Bmatrix} l_1 \\ 1 \end{Bmatrix} \mathbf{G}_{x_s}. \quad (\text{A-5})$$